GLACIERS AND FLOODING IN HIMALAYAN RIVER BASINS

JAMES RISING

ABSTRACT. As part of a project to study the economic effects of flood disasters in Pakistan, this research explores the contribution of glaciers to flooding throughout the Himalayan river basins, and how this glacier effect will evolve with climate change. Estimates of the precipitation and melt contributions to the Pakistan 2010 flood are presented, as well as the total volume based on satellite photos (55.2 ± 1.1 km^3). An analytic model of the stochastic contributions to flood risk is developed and applied to historical and predicted weather in Pakistan. *Additional estimates of the precipitation and melt contributions to the Pakistan 2010 flood, and the increase in expected size of a 100-year flood based on temperature changes will be included.*

1. INTRODUCTION

This research proposal is drafted like a research paper, to show both my current progress and plans for future research. All of the results shown are preliminary, some results need serious revisiting, and some untenable simplifications are used, all which I try to call out in the document. In particular, comments in this typeface represent planned future work. [**TODO:** NOTES IN THIS TYPEFACE REPRESENT MINOR CORRECTIONS TO EXISTING RESULTS WHICH COULD NOT BE COMPLETED BEFORE THE DEADLINE.]

Throughout the Himalayan river basins, flooding has become increasing problematic over the past couple decades, and in many areas the magnitude and frequency of severe floods is expected to increase further with climate change (Monirul Qader Mirza, 2003, Mirza et al., 2003). The role that glacier melt plays in flooding is still very uncertain, but the general trend is clear: the IPCC warns, "Glacier melt in the Himalayas is projected to increase flooding, and rock avalanches from destabilized slopes, and to affect water resources within the next two to three decades. This will be followed by decreased river flows as the glaciers recede" (Parry, 2007).

I have CRED EM-DAT in a fairly easily analyzable form, and it would be interesting to see (a) if Himalayan basin countries are outpacing other countries for flood disasters compared to this historical norm (and normalized for size somehow), and (b) how floods compare to other disaster types that are also exacerbated by climate change.

Pakistan has been subject to progressively increasing flood risk in recent decades (see figure 1), culminating in the recent 2010 flood, which affected 20 million people (Cross, 2010). These events reverberate throughout an economy, and identifying how their likely magnitude and frequency will change as glaciers melt will help governments plan their infrastructure development.

This research attempts to distinguish between the effects of glacial melt and changing precipitation patterns on flood frequency and nature. Because these factors will change very

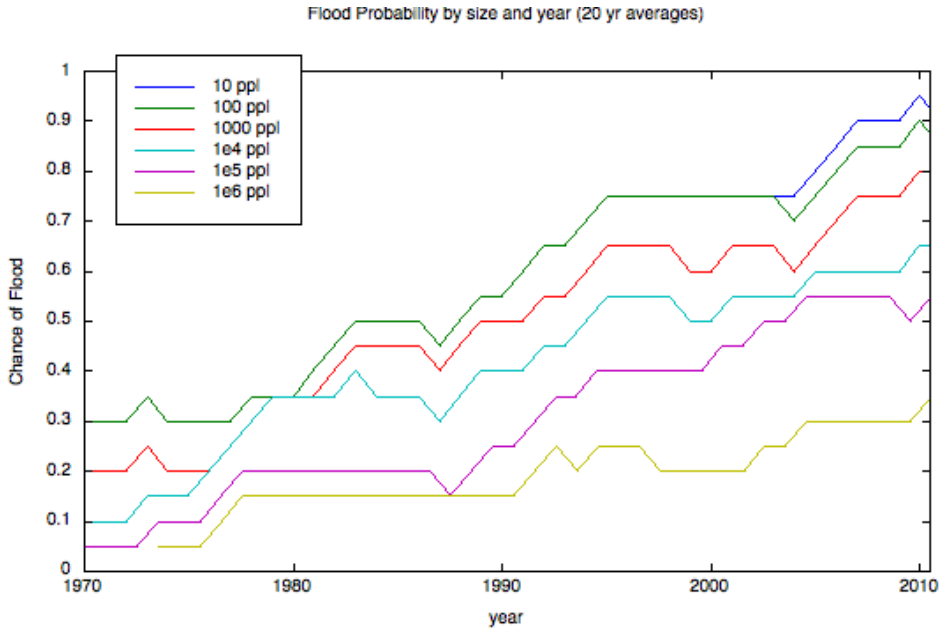

Figure 1: *Chance of Flooding in Pakistan:* Probability of floods of at least a given size in each year, as running 20-year averages. The size of the floods are based on number of people affected, on a log scale (green for 10 people, yellow for 1 million people). Source: CRED EM-DAT database.

differently over the next 50 years, an estimate of how flooding will change in time requires separate consideration of these two partial effects. The goal of this paper is to identify the contribution that glaciers make to floods in river basins of the Himalayas, and to estimate how flood probabilities will change in time, as climate changes and glaciers melt.

The approach is three-fold. First, the basic magnitudes of glacier contributions to flooding are explored, through the relevant literature and numerical studies. Second, an analytic model is developed to describe the relevant dynamics and factors that affect flood probabilities. Third, the assumptions of the analytic model are tested for the Indus river basin, and the model is applied.

2. Background Literature

The region of interest contains both the Himalayas, which feed the Indus and Ganges-Brahmaputra basins, and the Tibetan Plateau, which feeds the Salween, Mekong, Yangtze and the Huang He rivers. See figure 2.

Glaciers in this region have a wide variety of temperature profiles, ambient annual temperatures, and ablation characteristics, leading authors to a variety of classification schemes (Huang, 1990). However, because of the monsoon regime, these glaciers share some peculiarities, including simultaneous accumulation and ablation in summer (Ageta, 1983), and in many cases more rapid retreat than glaciers in other regions of the world (Fujita et al., 1997). A growing body of literature examines the implications that this glacier retreat will have on water availability for the 50-60% of the world's population that relies on glacier

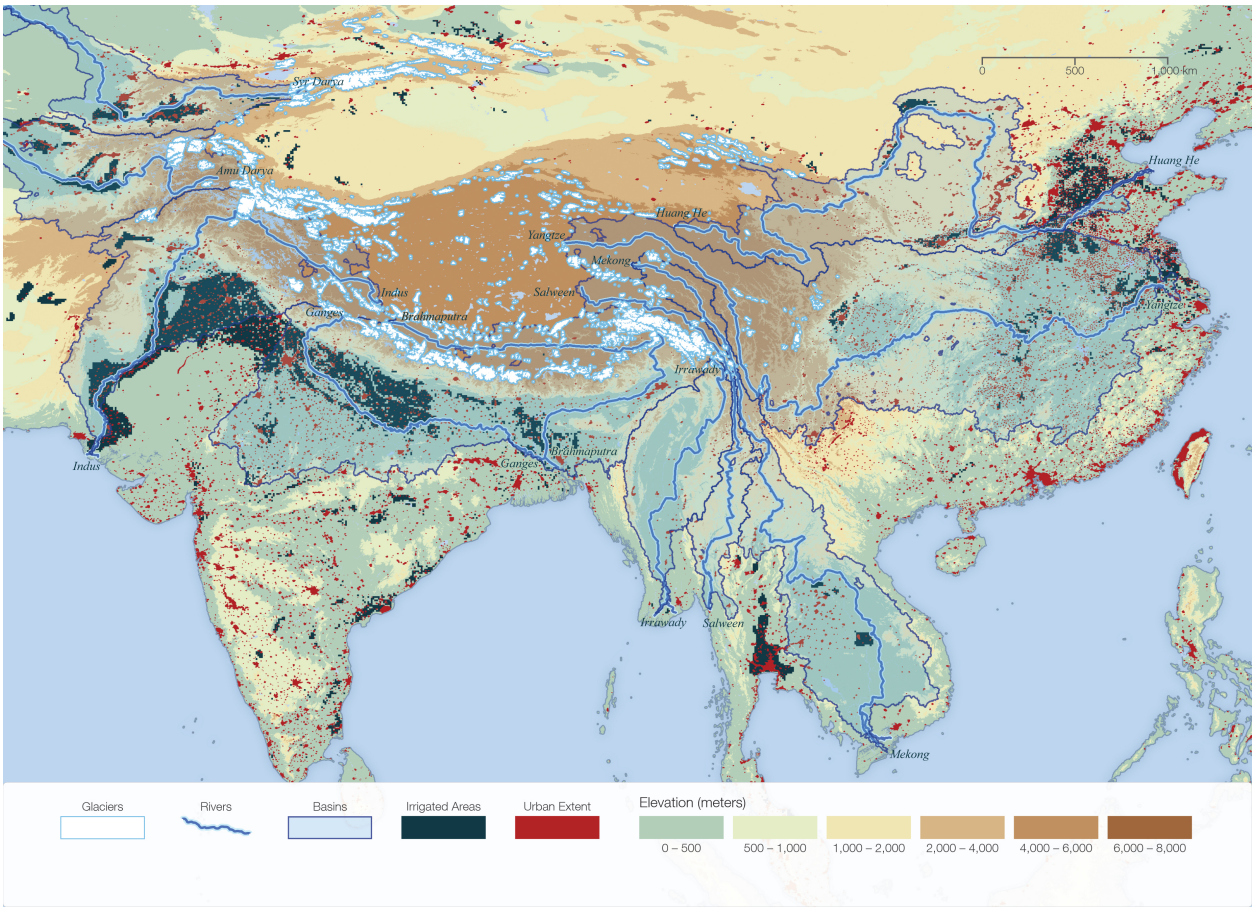

Figure 2: *Himalayan Basin:* This map shows major glaciers, rivers, river basins, and urban centers, as of June 2009. Courtesy of CARE International and CIESIN at the Earth Institute of Columbia University.

runoff, but since as much as 70% of river water in the summer months is due to ice and snow melt (Barnett et al., 2005), glaciers can also affect drainage river flood dynamics.

The climate change profiles for this region predict significant increases in annual temperatures, total precipitation, and the prevalence of extremely warm and wet seasons (see table 1). All of these will contribute to flood risk, through greater precipitation runoff and melt runoff. In particular, temperatures are likely to uniformly increase, but the effect on precipitation shows a less clear trend (see figure 3), and studies of actual precipitation trends are inconsistent across southern Asia (Cruz et al., 2007). Extreme weather events are also expected to increase (see figure 4), which will increase the propensity for disasters. Finally, greater winter accumulation is predicted in some regions (Dyurgerov et al., 2005), which combined with a sharp seasonal temperature transitions may result in significant additional runoff and increases in the variability of runoff. However, the complexity of mountain topography makes modeling the effects of climate change unreliable for much of this area (Solomon et al., 2007, Box 11.3: Climatic Change in Mountain Regions).

	Temp. Response (°C)			Prec. Response (%)			Extreme Seasons (%)		
Season	25%	50%	75%	25%	50%	75%	Warm	Wet	Dry
Southern Asia (5N,64E to 50N,100E)									
DJF	3.2	3.6	3.9	-9	-5	1	99		
MAM	3.0	3.5	3.8	-2	9	18	100	14	
JJA	2.2	2.7	3.2	**4**	**11**	**16**	96	32	-1
SON	2.5	3.1	3.5	**8**	**15**	**20**	100	29	-3
Annual	2.7	3.3	3.6	**4**	**11**	**15**	100	39	-3
Tibetan Plateau (30N,50E to 75N,100E)									
DJF	3.7	4.1	4.9	**12**	**19**	**26**	95	40	0
MAM	2.9	3.6	4.3	**4**	**10**	**14**	96	34	-2
JJA	3.2	4.0	4.7	0	4	10	100	24	
SON	3.3	3.8	4.6	-4	8	14	100	20	
Annual	3.2	3.8	4.5	**2**	**10**	**13**	100	46	-1

Table 1: *Global model projections:* Combined results of 21 global models under the IPCC's A1B scenario. Changes are between the 1980-1999 average and the 2080-2099 average. The table shows 25%, median, and 75% quartiles among the models for temperature and precipitation. Precipitation numbers are in bold when all models in the middle half of the resulting distribution are of the same sign. Extreme seasons are only shown when 2/3 of the models agreed. Adapted from the IPCC's AR4 Working Group I report, chapter 11 (Solomon et al., 2007).

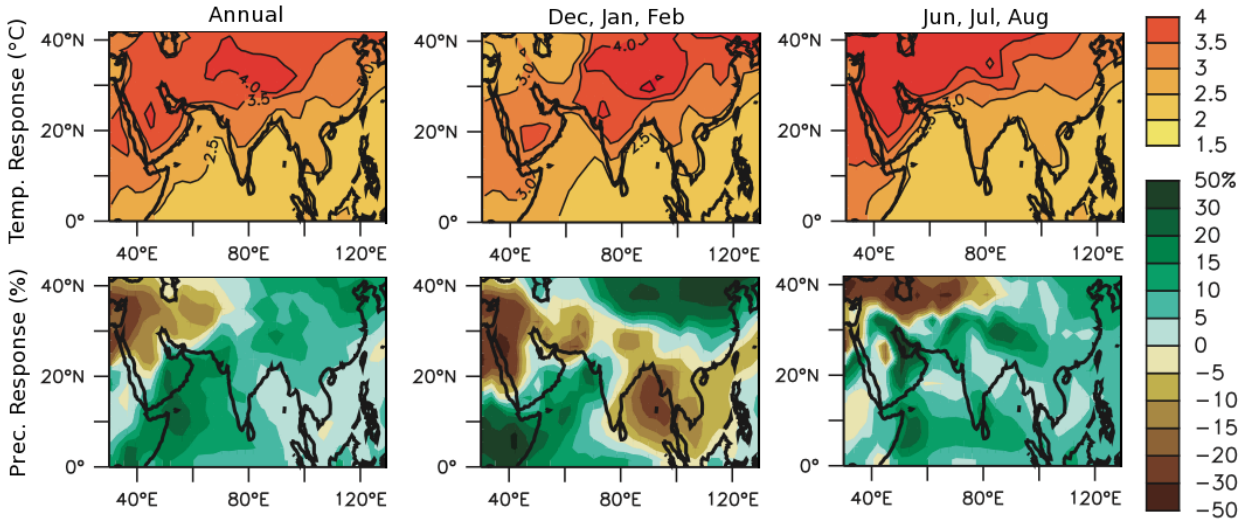

Figure 3: *Temperature and precipitation changes:* Changes between 1980-1999 average and the 2080-2099 average, according to the IPCC's MMD-A1B scenario, averaged over 21 climate models. Adapted from the IPCC's AR4 Working Group I report, chapter 11 (Solomon et al., 2007).

Two areas of research have approached the questions of this paper: the effects of glaciers on streamflow and water availability vis a vis climate change, and the holistic modeling of floods.

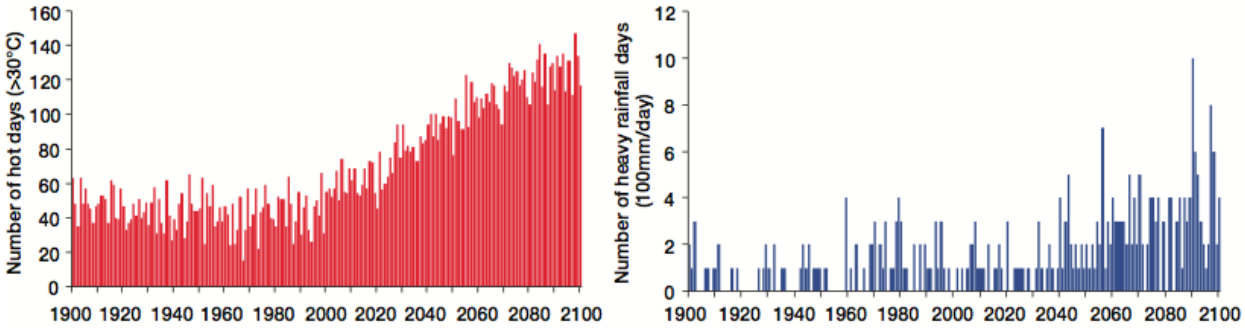

Figure 4: *Extreme Events:* Projected number of hot days ($> 30°C$) and days of heavy rainfall ($>$ 100 mm/day), reproduced from Cruz et al. (2007) (source: K-1 coupled model (MIROC), Hasumi and Emori, 2004).

Energy and mass balance calculations are typically used to model glacier growth and retreat, although temperature has been shown to be a reliable proxy for these (Ohmura, 2001). Kaser et al. (2003) gives an overview of the basic relationships of glacial runoff. One relevant result from his paper is that glaciers can buffer precipitation (smoothing precipitation peaks), so a decrease in glaciation area, and not just the melt it causes, might result in a increase in flooding.

Several researchers have focused on the effects of climate change on the Himalayan hydrology (Fujita et al., 2007, Singh and Kumar, 1997, Dairaku et al., 2008), but very few studies have tried to model the effects of climate change on flooding. Singh and Bengtsson (2005) provides an excellent model of streamflow in the Himalayas, though not one that accounts for climate change or flooding. Monirul Qader Mirza (2003) discusses the effect of peak flow sinchronization, lag-times, recession times, return periods, and provides a deep analysis of the 1987, 1988, and 1998 floods. Mirza et al. (2003) knits together hydrology models and climate change models to attempt to identify changes in floods that can be expected by climate change.

Since the catastrophic Khumbu Himal flood in 1985, Glacial Lake Outburst Floods (GLOFs) have been an active topic for research (Kattelmann, 2003). Within 10 km of the GLOF source, discharge (streamflow) from the GLOF can reach 60 times the corresponding maximum seasonal high flow flood discharge, but it drops with distance (Desloges and Church, 1992, Cenderelli and Wohl, 2001). The decrease of the GLOF/seasonal discharge ratio is the combined result of the attenuating effects of the mountain shadow on monsoon precipitation and small cumulative drainage area, and the increasing losses due to friction from silt and debris. Typically, GLOF flood waves dissipate within 30 km of their source, but a large GLOF can maintain a destructive wave for over 200 km (Richardson and Reynolds, 2000).

Finally, the implications of flooding have been discussed by many authors. Ahern et al. (2005) provides a survey of the epidemiological effects of flooding, while Kundzewicz and Takeuchi (1999) provide an overview of the history of flood control and mitigation, and suggest the idea of "living with floods." The framework for how to manage the hydrological effects of climate change needs considerable development (Wescoat Jr, 1991).

A wide variety of methods for quantifying flood return times have developed since the seminal rigorous approaches by Gumbel (1941) and Todorovic and Zelenhasic (1970). However, these methods require a closer look, both from mathematical and a data-driven standpoint (Kidson and Richards, 2005).

While the results of this paper are variously based on or inspired by accepted principles in the scientific literature, I should familiarize myself with foundational books like Maidment and Koch (1993) before too long.

3. Flood Magnitude

A number of metrics could be used to describe the magnitude of a flood. Perhaps the most natural is area flooded, although this can be difficult to model even with a detailed topographical map. The most frequent is streamflow, in either cusecs or m^3/s, on the principle that a flood is essentially a river that is flowing too much. See the next section for some rough calculations of streamflow. Other possibilities include people affected or displaces, and economic damages, neither of which correlate very well with hydrological magnitudes. [**TODO:** create a graph of # affected and economic costs from EM-DAT, showing don't correlate with eachother] .

A prior magnitude produces all of the above: the sheer volume of water with which a basin is innundated. This is the metric this study will focus on.

3.1. Discharge Comparisons.

A brief back-of-the-envelope calculation can help motivate this work. Consider Reach L8 from Cenderelli and Wohl (2001), a point on the Dudh Kosi river. This reach, at 2580 m, serves a drainage basin of 1151 km^2. Seasonal high flow floods produce peak flows of 205 m^3/s. The calculation for melt discharge is approximately $Q = \mu AT$, where μ is the degree day factor, A is the drainage area, and T is the mean temperature. If $\mu = 5$ mm / day °C (Hock, 2003), and $T = 3$°C, the difference predicted by Solomon et al. (2007), then $Q = 200m^3/s$– that is, an doubling of the peak seasonal flow. In comparison, at Reach L8, a 1985 GLOF produced a total discharge flow of 1375 m^3/s. Streamflow from precipitation scales with drainage basin area, and snow melt scales with snow-covered area, while GLOFs do not scale and glaciers only scale with roughly the square root of the area.

3.2. Drainage Model.

A basin drainage model will support a variety of work within this research, and will be described in general here and applied to the esimates and used for statistical tuning. The drainage model consists of (1) a simplified model for a drainage basin, divided into strips representing the time that runoff takes to flow the drainage point, and (2) a hydrograph-style linear system to transform precipitation and temperature data into streamflow. These models will be used to estimate the precipitation that contributed to the Pakistan 2010 flood, as well as provide the necessary framework for matching recent gridded precipitation data with historical station data to fit the statistical model presented later.

An accurate topography of the Indus basin is essential for modeling the drainage basin. This reseearch uses the NOAA NGDC's Global Land One-km Base Elevation (GLOBE) Digital

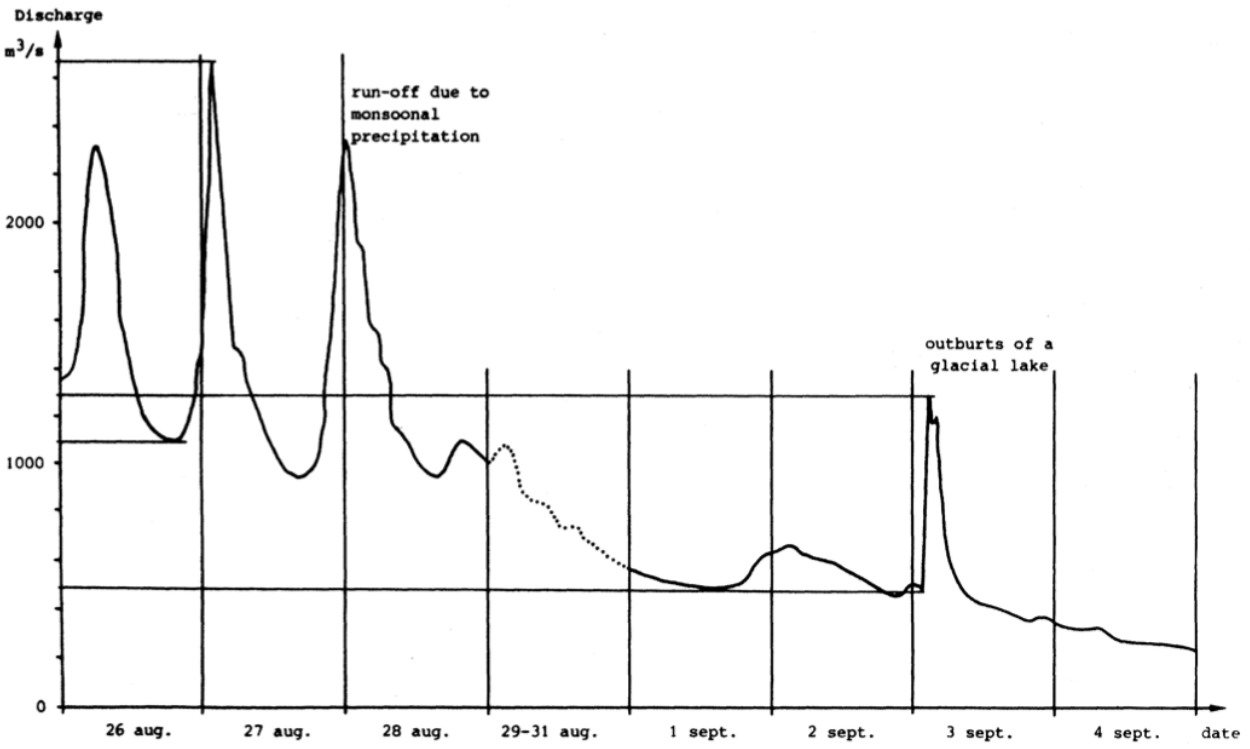

Figure 5: *Relative discharge rates:* Discharge hydrograph of the Dudh Kosi at the Rabuwa Bazar station, about three times as far from the source of the 1985 GLOF as Reach L8 mentioned in the text. Reproduced from Zimmermann et al. (1986), source: Dept. of Irrigation, Hydrology and Meteorology, His Majesty's Government of Nepal, Kathmandu.[2]

Elevation Model. This provides a spacial resolution of 1km x 1km, and 1 meter elevation resolution (but with inaccuracies, described below, see figure 10).

See figure 6 for the basin map. This is constructed by determining the path for water precipitated on each grid cell, and identifying those paths that flow through the drainage point (white cell in the figure).

The time taken for water to flow is determined using Manning's Forumla, $V = \frac{1}{n} R_h^{2/3} S^{1/2}$. V is the flow velocity in m/s. n is .033 s / $\mathrm{m}^{1/3}$, an average value for natural rivers. R_h is the hydraulic radius, which is modeled as increasing linearly over the course of the basin. For the Indus river basin, it is taken as starting at 1 m and increasing by 1 mm per km to reflect the total discharge of 6600 m^3/s over a path of 3000 km and a drop of 4627 m. That is, Manning's forumla, multiplied by cross-section $s = 1$ km and depth d, and set equal to the total discharge rate, can be used to solve for the average depth:

$$6600 m^3/s = \frac{(1000m)d}{.033 s/m^{1/3}} d^{2/3} (4627m/3000km)^{1/3} \implies d = 1.5m$$

As noted in the formula, the speed of water depends significantly on its depth. As the flood builds, the water flows faster. I need to figure out some way to map a parameter other

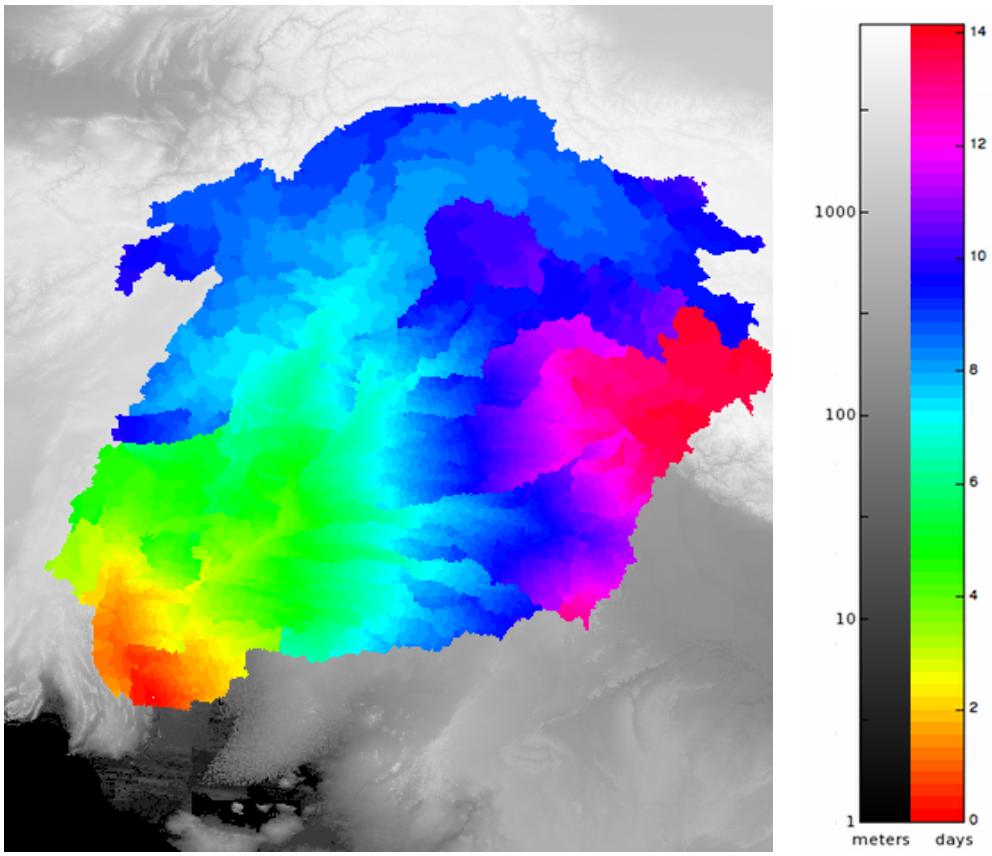

Figure 6: *Basin Map:* Colors show the number of days runoff takes to reach the drainage point, based on Manning's Formula and the topography.

than days, which can then be used to calculate travel times for other parts of these calculations.

Applying precipitation and temperature data to this basin model requires a simple hydrological model. The goal of the numerical model is to translate observed input data (precipitation, temperature, and topography) into observed resulting magnitudes (streamflow). The model below provides considerable power with sparce information, but opportunities to improve it abound. In particular, the energy-balance equations from Fujita and Ageta (2000) were designed for the monsoon climate and would improve glacier melt model. The numerical model of basin flow used by Higashi and Matuura (2006) would further improve the results.

The numerical model is informed by the following variables:

(1) $P(t, x, y)$, the precipitation, in $\frac{w.e.}{m^2 hr}$ (water equivalent per area per hr).

(2) $T(t, x, y)$, the temperature, in $^\circ C$.

(3) $\xi(x, y)$, the elevation at a point

(4) $\mu_s(\xi)$ and $\mu_i(\xi)$, the melt coefficient of snow and ice at levels of altitude, in $\frac{w.e.}{^\circ C hr}$. The coefficients are used to determine snow and ice melt by a temperature-index method,

suggested by Ohmura (2001), and estimated at different altitudes using the results in Kayastha et al. (2003).

Below, $\mathbf{1}\{\cdot\}$ is the indicator function, with a value of 1 where $\cdot$ is true, and 0 otherwise. Define the snow melt at a point, $M_s(t,x,y)$, as a linear response to temperature, and total snow depth, $S(t,x,y)$:

$$M_s(t,x,y) = \mu_s(\xi(x,y))T(t,x,y)\mathbf{1}\{T(t,x,y) > 0, S(t,x,y) > 0\}$$

$$S(t,x,y) = \int_{-\inf}^{t} P(\tau,x,y)\mathbf{1}\{T(\tau,x,y) \leq 0\} - M_s(\tau,x,y)d\tau$$

Analogously, define the glacier melt, $M_i(t,x,y)$ and glacier height $G(t,x,y)$.

$$M_i(t,x,y) = \mu_i(\xi(x,y))T(t,x,y)\mathbf{1}\{G(t,x,y) > 0, T(t,x) > 0, S(t,x) = 0\}$$

$$G(t,x,y) = \int_{-\inf}^{t} -M_i(\tau,x,y)d\tau$$

Streamflow is composed of delayed contributions from along the whole length of the stream. If the flow over time at $x = x_0$ is $q(t)$, that flow contributes to the flow at location downstraem $x = x_0 + \Delta x$ as $q(t) \star d(t, \Delta x)$ (the convolution is taken along the time dimension). Because the precipitation and temperature data are on a daily basis, the calculation is done on a daily basis: M_i and M_s are calculated throughout the basin, and at each point, (x,y), they contribute to the total streamflow. This flow is then allowed to progress from each basin region forward one day closer to the drainage point, according to the basin model. Then the aggregate flow within region D is

$$Q_d(t) = \iint_D (P(t,x,y) + M_s(t,x,y) + M_i(t,x,y))\mathbf{1}\{T(t,x,y) > 0\}\mathrm{d}x\mathrm{d}y + Q_{d+1}(t) \star d(t)$$

(here the subscript of Q_d increases moving away from the drainage point, and Q_0 is the flow through the drainage point.)

For modeling the delay function $d(t)$, which is a partial hydrograph, consider the response of a basin to a unit impulse of rain over an entire basin at time $t = 0$, $\delta(t)$. Example unit hydrographs are given in figure 7. Given the range of theoretical options, a simple step function is used:

$$d(t) = \frac{1}{2}\left[u(t-2) - u(t)\right]$$

$u(\cdot)$ is the unit step function, and the span of the function is chosen so that the average delay is 1 day.

3.3. **Pakistan Flood Size.** I estimate the volume of the Pakistan flood of 2010 in two ways: by estimating the volume of the flood water from satellite photos, and by identifying how much precipitation is recorded upon the Indus flood basin during the relevant storm. The hope is to attribute the difference between these two volumes to the glacier contribution, evaporation, and seepage, if error in the coarseness of the calculation data is small enough.

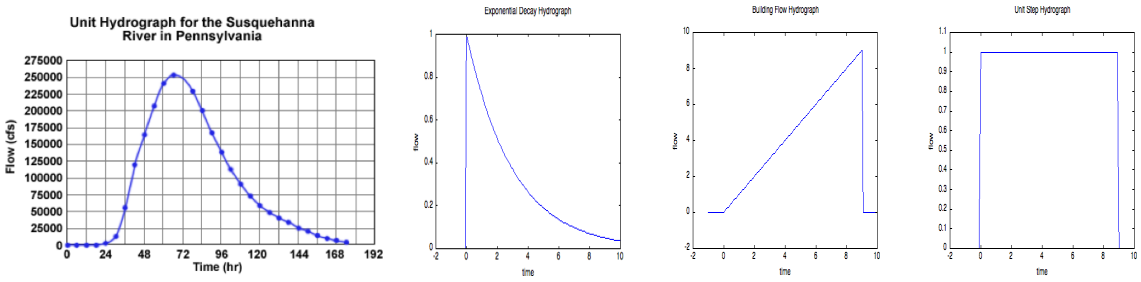

Figure 7: *Unit Hydrograph Examples:* A shows a real unit hydrograph from `http://www.meted.ucar.edu/hydro/basic/UnitHydrograph`. B shows an exponential decay, suggested by figure 5. C show a sawtooth effect, which would result from a basin shaped like an extruded V: as the excess flow comes from higher up the basin, it builds. D show the hydrograph used in this model.

The basin model is used from the previous section, based on NGDC GLOBE data. Precipitation data is from NASA's Tropical Rainfall Measuring Mission (TRMM), algorithm 3B42, which has .25° x .25° spacial resolution (about 28 km on a side).

The calculation of flood volume from area involves six steps:

(1) **Identify flood extent**: The flood extents are from the *Spatio-Temporal Flood Analysis along the Indus River, Sindh, Punjab, KPK and Balochistan Provinces, Pakistan* from ICIMOD and SERVIR Himalaya based on the daily MODIS Terra and Aqua datasets. Each day's extent is denoted in a specific color, so each color denotes a mask. Four colors are used to make the total flood mask, corresponding to the normal Indus river coverage, the first day flood coverage, and the two colors used to denote grid cells that contain seasonal minor rivers and the normal or first day coverage.

(2) **Clean the extent data**: The ICIMOD map contains annotations and roads which obscure the flood. The flood results are smoothed by adding to the mask wherever the majority of the surrounding pixels are set.

(3) **Match between maps**: The ICIMOD map is drawn on a slant, and at a different scale from the GLOBE topography. Four locations were chosen as points of correspondence between the two maps. See figure 8.

(4) **Calculate cell areas**: Cells are identified by latitude and longitude, which allows them to vary in actual area by around 8%. The area of each cell is individually calculated.

(5) **Approximate water height**: Using numerical methods, flood elevations above the topography are assigned to each flood pixel in the satellite image. Since the water cannot be assumed to be stationary, its height can only be approximated. The two rules used for doing this are (a) the height of the flood at its boundary is 0, and (b) between grid cells, the height of the land topography plus the flood waters should be as similar as possible. See figure 9.

(6) **Multiply depths by areas**: The result is 55.2 ± 1.1 km^3 of water. The lower bound was calculated by smoothing the terrain by up to 1 m, and removing a 10

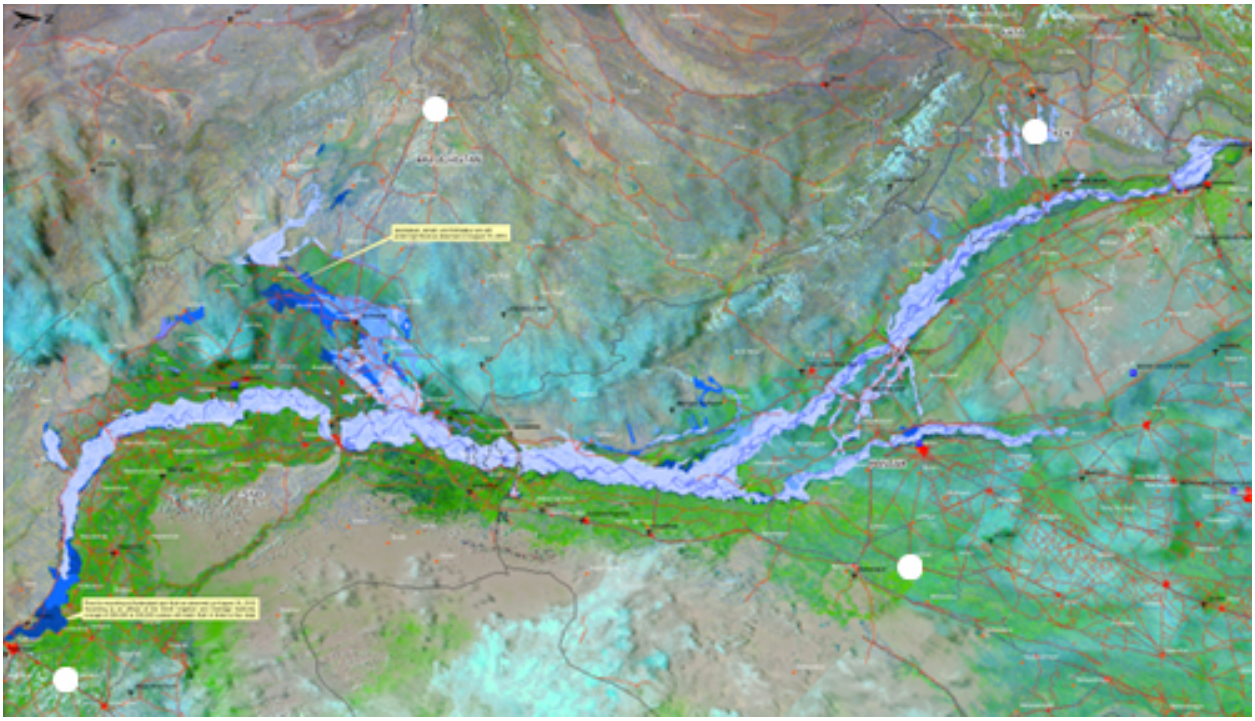

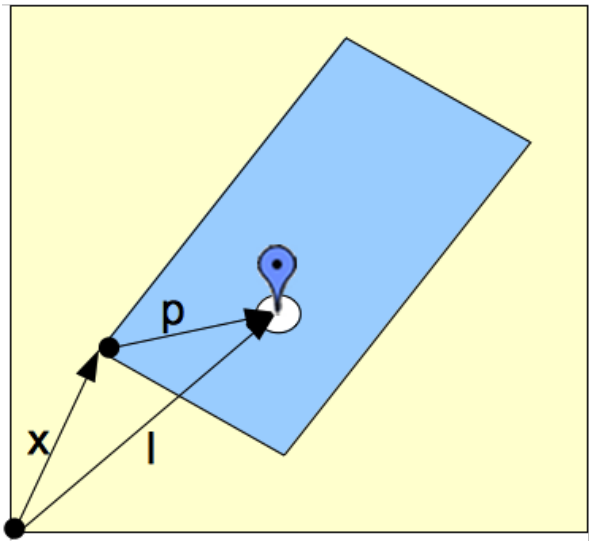

$$\begin{pmatrix} x_{long} \\ x_{lat} \end{pmatrix} + \begin{pmatrix} A_{11} & A_{12} \\ A_{21} & A_{22} \end{pmatrix} \begin{pmatrix} p_{long} \\ p_{lat} \end{pmatrix} = \begin{pmatrix} l_{long} \\ l_{lat} \end{pmatrix}$$

Location	**Latitude, Longitude**	**Pixel X,Y**	**Excluded** x_{long}, x_{lat}	**Excluded** $A_{11}, A_{12}, A_{21}, A_{22}$
Tando Allahyar	25.468074 N 68.716908 E	243, 2715	65.511894 N 28.110763 E	0.001081, 0.001070, 0.001081, -0.001074
Kahror Pakka	29.630324 N 71.89702 E	3660, 2268	65.506109 N 28.108937 E	0.001081, 0.001086, 0.001081, -0.001069
Gara Hayat	32.050935 N 70.573339 E	4164, 522	65.524038 N 28.114598 E	0.001072, 0.001080, 0.001078, -0.001071
Sibbi	29.531794 N 67.864437 E	1746, 434	65.559755 N 28.125878 E	0.001070, 0.001067, 0.001077, -0.001075
Average			65.525449 N 28.115044 E	0.001076, 0.001076, 0.001079, -0.001072
RMS Error			0.0208, 0.0066	0.000005, 0.000008, 0.000002, 0.000002

Figure 8: *Matching between maps:* The first two maps shows the four points of correspondence between the flood extent map and Google's map (intersections of major roads).

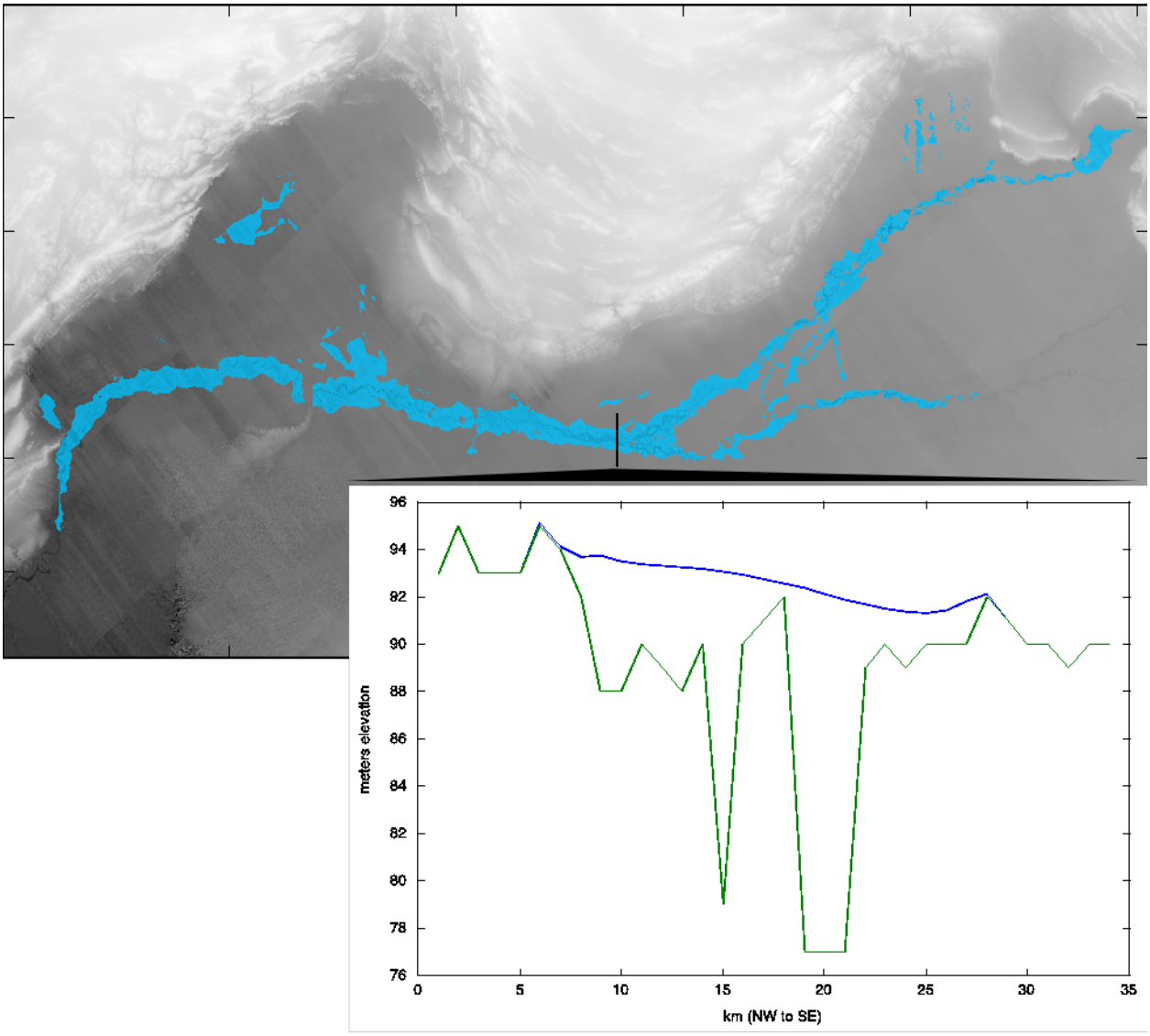

Figure 9: *Flood Mapping:* The map shows the togography corresponding to the ICIMOD map, the extent of the flood on August 15, and the calculated depths of the flood (light shading on flood extent). The selected cross-section shows how the flood lays on the land togography.

cm minimum flood requirement. Elevation data appears to be reliable over the flood extent map; see figure 10.

The calculation of precipiation volume proceeds as follows:

(1) **Determine daily masks**: Starting with the flood extent map above, record a unique "applicable basin" mask for each day by extending outward from the previous day's mask by one day, according to the basin model. The first (smallest) mask is mask denotes the area of precipitation that could contribute to the flood on the last day, the second mask is for the second-to-last day, and so on.

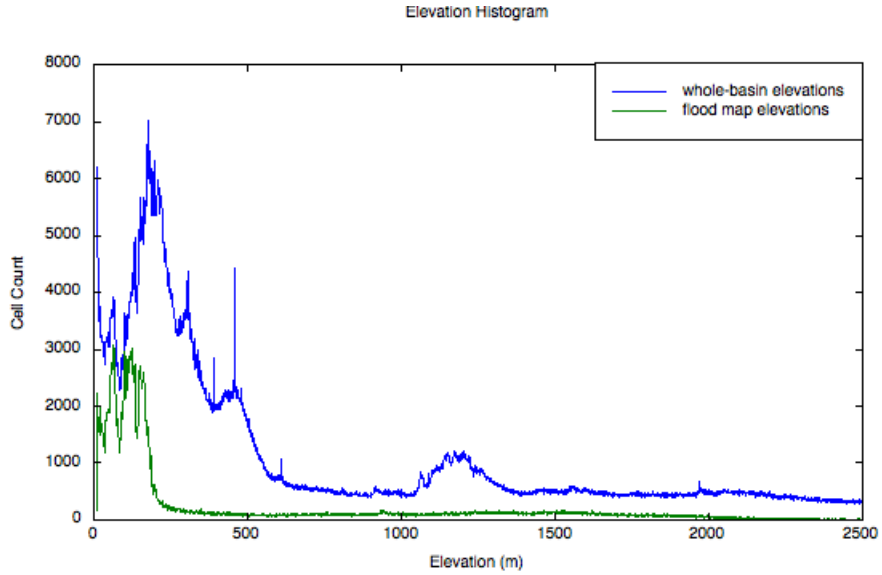

Figure 10: *Elevation Histogram:* The GLOBE DEM data was derived in part from cartographic sources, which can result of contour line artifacts, and has the potential for up to ± 250 m errors. Applying the same criteria as the GLOBE report, this histogram identifies elevation data artificats (see `http://www.ngdc.noaa.gov/mgg/topo/report/plates/p27a.html` for the histogram for Southeast Asia). There are clear spikes near 300 m, 390 m, and 450 m, reflecting topographic artifacts (blue line). However, these are absent from the flood section (green line).

(2) **Aggreagate daily precipitiations**: *This still needs to be done, as well as a range estimation. Instead, the following are total basin precipitation estimates:* As a comparison, the total precipitation that fell on the basin was calculated, based on the precipitation cell areas (which vary between around 600 km^2 and 720 km^2 for each precipitation cell). The result is 1.18e8 mm km^2 = 118 km^3. [**TODO:** Add a range estimation]

One important aspect of the Pakistan 2010 flood is the range of days over which there was ample precipitation– from July 1 to mid August. Note in figure 11 that although greater single-day precipitation totals have occurred over the past decade, this has been the highest average precipitation over a month. This causes problems for predicting the behavior of water, as the ground it is running over changes.

There appears to be a problem in either the TRMM data or the IRI/LDEO interface to it, such that there is no precipitation recorded for most of August and September. I don't know why this is, but it potentially misses half of the storm event.

The next step is to use temperature data over the span of the flood event to estimate the predicted glacier melt that contributed to the flood.

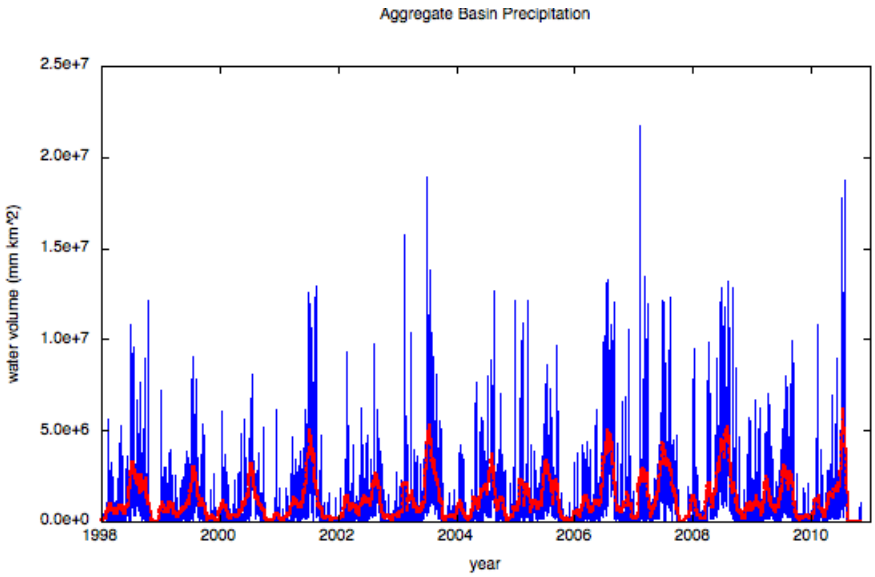

Figure 11: *Aggregate Basin Precipitation:* Total basin precipitation volume (blue), and 30-day running averages (red). Note that the 2010 average precipitation is higher than previous years, although two previous years had higher day precipitation totals.

4. Analytic Model

The goal of the analytic model is to capture the approximate the stochastic relationships involved in flooding. In particular, by describing the distinct roles of melt and precipitation on flooding, it will support a model of flood probabilities changing in time.

Recently flood frequency analysis has experiences a proliferation of statistical models (Kidson and Richards, 2005). The analysis below attempts to make minimal assumptions that capture the distinct effects of precipitation and melt.

Consider a basin drained to a point, and we wish to determine the contributions that form the streamflow at that point. Let temperature across the basin be approximated by a weak-sense stationary (WSS) random process, $T(t)$, near a point in time. Furthermore, let it be normalized to a mean of 0, and have autocorrelation function $R(\tau)$. As a first-order approximation, let

$$R(\tau) = \begin{cases} 1 - \frac{|\tau|}{w} & \text{for } -w \leq \tau \leq w \\ 0 & \text{otherwise} \end{cases}$$

See 12.

The effect of temperature on streamflow is the integral of this temperature random process, weighted by a function, $a(t)$, which captures the effect of the basin on upstream flow contributions (e.g., where glaciers reside and their average melt coefficients). Note that here $T(t)$ is not the temperature at the drainage point. Instead, $T(-s)$ is the temperature a certain distance up the basin, such that over time s, the water will run down to the drainage point. Since not all points a time-distance s away will have the same temperature or the same melt

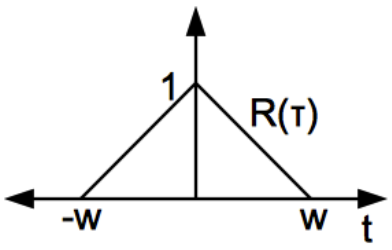

Figure 12: *WSS Autocorrelation:* $R(\tau)$ drops linearly from an autocorrelation of 1 at $\tau = 0$ to 0 for $\tau \geq w$

coefficient, and not all of the water thereby melted reach the drainage point at a uniform time, $a(t)$ is an empirical approximation. See figure13.[3]

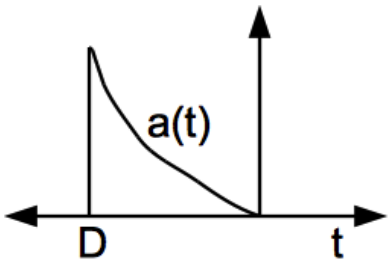

Figure 13: *Temperature Streamflow Weighting:* $a(t)$ approximately captures the differences in temperature, melt factor, and drainage time of water throughout the basin.

Then, the streamflow due to temperature is

$$Q_T(t) = A\bar{T}(t) + \int_{-\infty}^{\infty} a(\tau, t)T(\tau)d\tau$$

Where $A\bar{T}(t)$ is the melt due to the average value of T, near time t. The variance of $Q_T(t)$ can be calculated only based on $a(t)$ and $R(\tau)$:

$$\begin{aligned} E(Q_T - A\bar{T})^2 &= E\int_{-\infty}^{\infty}\int_{-\infty}^{\infty} a(\tau, t)a(\tau', t)T(\tau)T(\tau')d\tau d\tau' \\ &= \int_{-\infty}^{\infty}\int_{-\infty}^{\infty} a(\tau, t)a(\tau', t)R(\tau - \tau')d\tau d\tau' \\ &= \int_{-\infty}^{\infty} b(v, t)R(v)dv \text{ where } b(v, t) = \int_{-\infty}^{\infty} a(\tau' + v, t)a(\tau', t)d\tau' \end{aligned}$$

Assume that the melt contribution has a normal distribution with mean $A\bar{T}$ and variance calculated above.

[3] I could perhaps more accurately capture the distribution of the integral of temperatures by simply sampling those values and fitting a curve, but this approach allows the multiplicative function, $a(t)$, to be distinguished from the temperature process.

In conjunction with this, let precipitation have a probability density function, $f_p(p) = \alpha\delta(p) + \frac{(1-\alpha)}{\rho}e^{-(p-p_0)/\rho}u(p-p_0)$ (see figure 14). This reflects that the actual probability distribution may be complicated, but below a certain sustained precipitation, p_0, the precipitation is irrelevant to flooding, and above that level, precipitation events follow an exponential distribution.

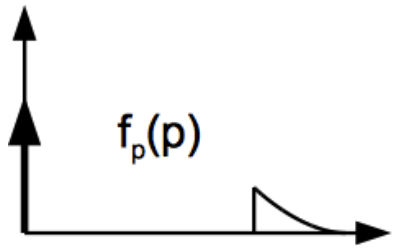

Figure 14: *Precipitation Probability Function:* $f_p(p)$ has most of its probability at $p = 0$, with the remainder as a decaying exponential starting at $p = p_0$.

The sum of precipitation (over the entire basin) and melt is approximately equal to the stream flow. We can calculate the size of the hundred year flood from by solving for q in $P(Q \geq q) = .01$. If streamflow due to melt is constant at $A\bar{T}$, then the size of a 100-year flood is given by,

$$\begin{aligned} P(\bar{Q} \geq q) &= \int_q^\infty \frac{(1-\alpha)}{\rho} e^{-\frac{p'-p_0-A\bar{T}}{\rho}} dp' = .01 \\ \implies q &= p_0 + A\bar{T} - \rho ln(\frac{.01}{1-\alpha}) \end{aligned}$$

However, if streamflow due to melt is a normal distribution with mean μ and variance σ^2, the size of a 100-year flood is given by,

$$\begin{aligned} P(\tilde{Q} \geq q) &= \int_q^\infty \frac{(1-\alpha)}{\rho} e^{-\frac{p'-p_0}{\rho}} \star n(\mu, \sigma^2) dp' \\ &= \int_q^\infty \int_{-\infty}^\infty \frac{1-\alpha}{\rho} e^{-\frac{p'-p''-p_0}{\rho}} \frac{1}{\sqrt{2\pi\sigma^2}} e^{-\frac{(p''-\mu)^2}{2\sigma^2}} dp'' dp' \\ &= \int_q^\infty \frac{1-\alpha}{\rho} e^{-\frac{p'-p_0}{\rho}} \int_{-\infty}^\infty \frac{1}{\sqrt{2\pi\sigma^2}} e^{\frac{-1}{2\sigma^2}[(p''-\frac{\sigma^2}{\rho}-\mu)^2-(\frac{\sigma^2}{\rho}+\mu)^2+\mu^2]} dp'' dp' \\ &= \int_q^\infty \frac{1-\alpha}{\rho} e^{-\frac{p'-p_0}{\rho}+\frac{1}{2\sigma^2}[(\frac{\sigma^2}{\rho}+\mu)^2-\mu^2]} dp' = .01 \\ \implies q &= p_0 - \rho[ln(\frac{.01}{1-\alpha}) - \frac{1}{2\sigma^2}[(\frac{\sigma^2}{\rho}+\mu)^2 - \mu^2]] \end{aligned}$$

For a range of parameters, this represents a significant increase in the size of the 100-year flood. See figure 15 for some numerical results.

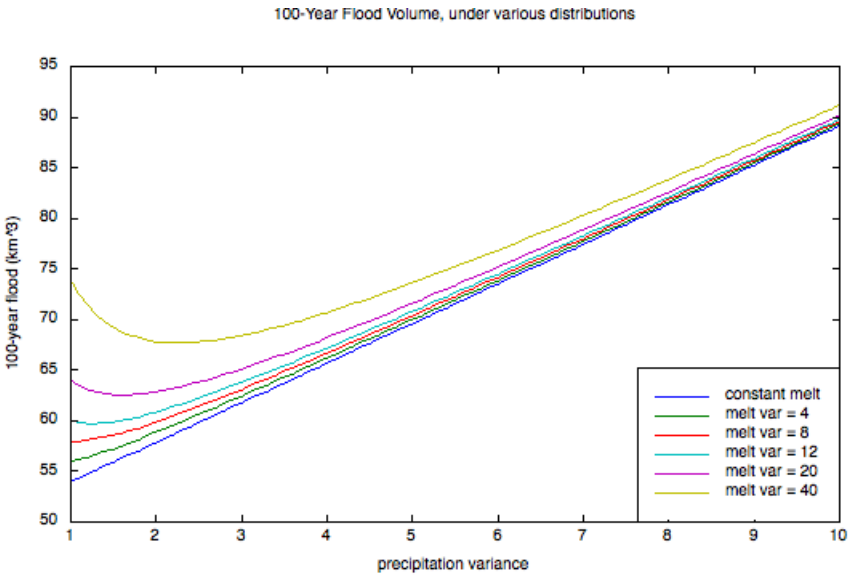

Figure 15: *100-Year Flood Volumes:* The graph shows expected 100-year volumes, given various variances in the precipitation and temperature melt, according to the model in the paper.

Note that this model does not account for GLOFs or cyclonic storms, which significantly affect the weather of parts of tropical Asia and have increased over the last half century (Farooqi et al., 2005).

The same model can be used to determine how more frequently a given baseline 100-year flood will occur, given parameters of climate change.

5. Application

The application of the model proceeds in two ways. First, I determine the yearly parameters, how these affect flood frequency and magnitude, and how these will evolve in time. Second, I determine daily parameters, how these will shift with climate change, and how that will affect agriculture. The two methods related by the following:

$$P(Q \geq q) = 1 - P(Q \leq q) = 1 - \prod_{d=1}^{365} P(Q_d \leq q)$$

where Q_d is a given day's precipitation model.

The application also needs to include checks that the assumptions of the model hold. Barnett et al. (2005) comments that a 33-38% increase in melt runoff is expected, and my parameters will hopefully reflect that.

5.1. **The Temperature Process.** Above, the temperature is taken to be a WSS random process, with a known autocorrelation function $R(\tau)$. Temperature is approximately stationary, with a constant mean and variance, only over the course of a short window of days, so $R(\tau)$ is determined by recalculating the mean and variance for overlapping blocks of days.

Let $X_T, X_{T+1}, \ldots, X_{T+n}$ by a small collection of n mean daily temperature values starting from time T, with mean μ_T and variance σ_T^2. Then, the partial autocorrelation for these values is

$$\hat{R}_T(k) = (X_T - \mu_T)(X_{T+k} - \mu_T)/\sigma_T^2$$

Over a larger range of N values, the total estimated autocorrelation is the average of these partial correlations,

$$\hat{R}(k) = \frac{1}{N-k} \sum_{T=1}^{n-k} \hat{R}_T(k)$$

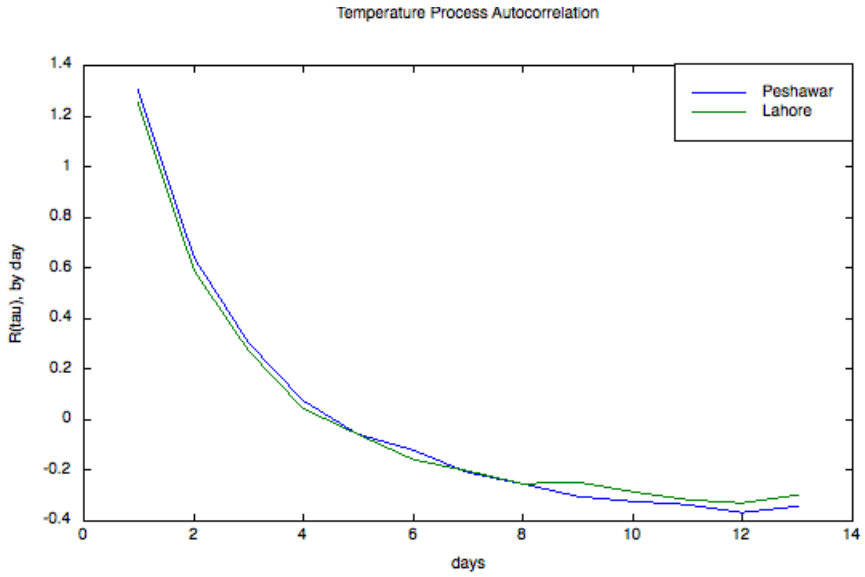

Figure 16: *Temperature Autocorrelation:* Two plots of average autocorrelation for locations near the northeast mountains: Peshawar at 34.0° N 71.6° E, and Lahore at 31.5° N 74.4° E.

The autocorrelation values above 1 come from the method of rolling blocks of autocorrelations, but are clearly undesireable. I need to find a way to eliminate them. Also, this is the autocorrelation for temperatures throughout the year, but floods only happen in the summer, so I can improve my temperature model by just considering the temperature process between certain dates.

Next, I need to estimate $a(t)$.

5.2. **The Precipitation Process.** Precipitation is merged from two sources: NOAA's Global Historical Climatology Network (GHCN) daily data for three stations in Pakistan (station 41620 in Zhob at 31.35 N, 69.47 E, station 61640 in Lahore City at 31.55 N, 74.33 E, and station 41560 near Parachinar, India at 33.87 N, 70.08 E), and gridded data from NASA's Tropical Rainfall Measuring Mission (TRMM), algorithm 3B42 over the entire basin. GHCN data is available from 1955 to 2004, while TRMM data is from 1998 to 2010. This provides 6 years of overlap for tuning parameters to calculate

$$Q_{TRMM}(t) = \sum_s \alpha_s P_s(t)$$

A more complete model would include temperature, and instead of using the total basin precipitation, would apply the basin model above to determine streamflow. The following model applies all of these elements, over a two week span:

$$Q_{TRMM}(t) = \sum_s \sum_{d=0}^{14} \alpha_{sd} P_s(t-d) + \sum_{d=0}^{14} \beta_d T_s(t-d) +$$
$$\sum_s \gamma_s \left(\sum_{d=0}^{14} T_s(t-d)\mathbf{1}\{T(t-d) > 0\}\right)\left(\sum_{d=0}^{14} P_s(t-d)\mathbf{1}\{T(t-d) < 0\}\right)$$

Historical precipitation is very sparse in this area. Although NOAA NCEP-NCAR has model predictions of precipitation, building a flood model on weather prediction data seems ill-advised.

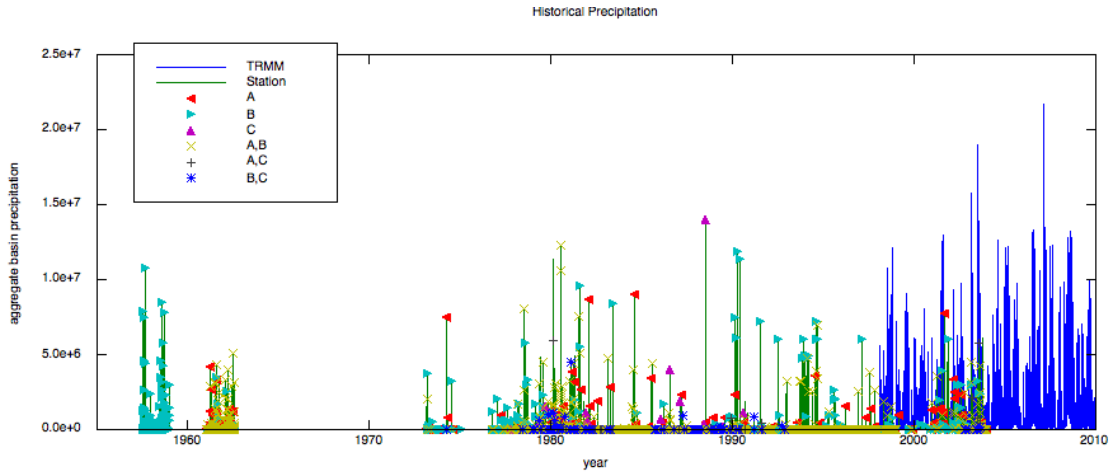

Figure 17: *Precipitation History:* Blue is the more reliable TRMM data. Green shows estimates of total basin precipitation based on station data. Each point is labeled by which stations were used to predict it: Stations A and B (RMS 1.7899e+06), stations A and C (RMS 1.6859e+06), stations B and C (RMS 1.0415e+06), station A only (RMS 2.0235e+06), station B only (RMS 2.1131e+06), or station C only (RMS 2.1448e+06). All three stations are not used together, because the overlap region did not contain any dates at which all three had non-zero precipitation values.

The following values were determined:

Regressed Stations	Coefficients	RMS Error	Overlap (N)	All Points	Additions
Station A only	1.5474e5	2.0235e6	457	3916	1191
Station B only	1.1974e5	2.1131e6	612	5770	2863
Station C only	1.0984e5	2.1448e6	39	389	97
Stations A and B	1.9041e5, 6.451e4	1.7899e6	325	2566	2069
Stations B and C	1.8656e5, 9.543e4	1.6859e6	34	260	54
Stations A and C	3.7336e5, 1.0151e5	1.0415e6	31	230	199

Since the δ-function is taken to capture all of the precipitation below a given level, p_0, a maximum likelihood estimate for both parameters fails by reducing the sample to a single

point. The problem with MLE is that it does not capture how well the data "fits" an exponential, just how likely each data point is, independently. Instead, an approach using moments is used. ρ for a given p_0 is given by

$$\rho = \frac{\sum_{p_i \geq p_0} (p_i - p_0)}{n}$$

where n is the number of points $\geq p_0$ (this is both the MLE and method of moments result), and then the given p_0 is scored by the second moment,

$$score_{p_0} = |Var(P_i) - \rho^2|$$

and the p_0 with a minimum score is used.

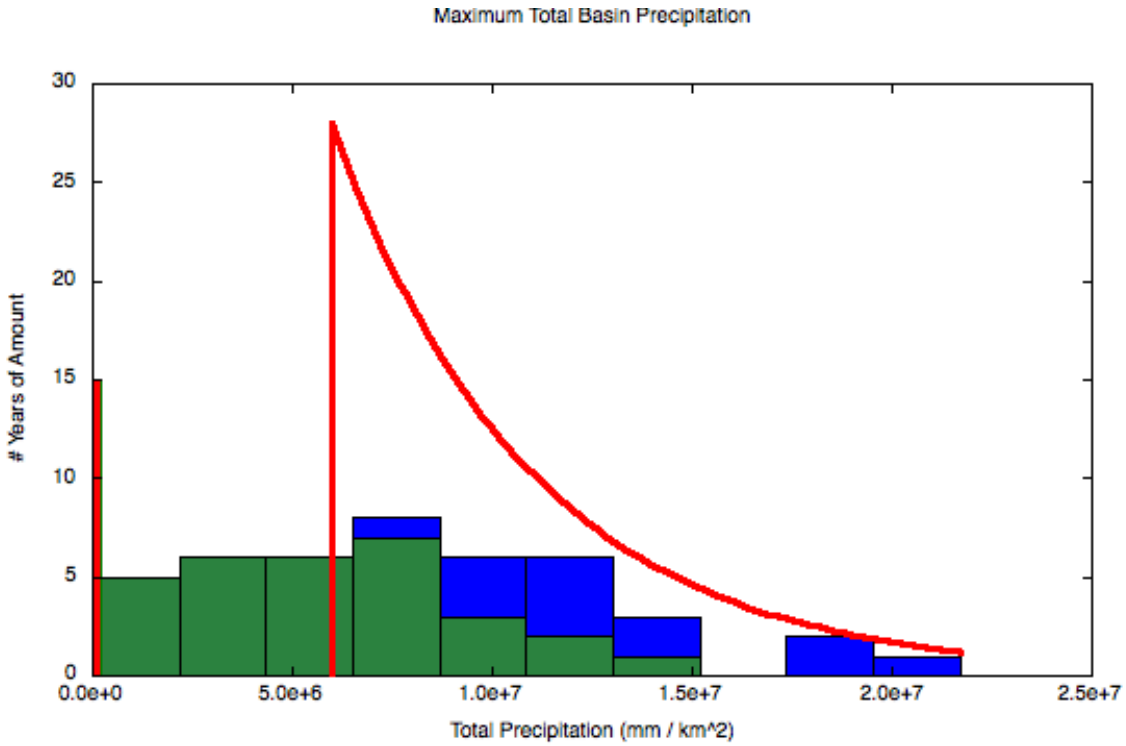

Figure 18: *Precipitation Model:* Blue is maximum basin-wide TRMM precipitations. Green is based on the station model. Red shows the resulting precipitation model for maximum yearly precipitation, scaled by 43 to match the histogram of 43 data points (the bar on the left should be a δ-function).

The result is $p_0 = 5.9871e6$, $\rho = 4.9883e6$, and $\alpha = .3488$ (28 of 43 maximum yearly precipitations are above p_0). *After I determine $a(t)$ for the temperature model, I can make 100-year flood predictions.*

Next I will apply this parameter tuning method on a daily basis, and identify the probability of a 100-year flood over the course of the year.

Finally, climate change estimates of changes in precipitation, temperature, and timing can be applied to these parameters to present how they will change over the next century.

The basin model can be tuned by comparing its flow estimates to http://www.bbc.co.uk/news/world-south-asia-10986220*, and the analytic model can be compared to* http://www.pakmet.com.pk/FFD/index_files/hpeak.htm *to generate better extreme-year estimates.*

6. Future Work

6.1. Additional Experiments.

- **What effects will seasonal flood timing shifts have on flood magnitude?** In particular, Barnett et al. (2005) notes that the seasonal peak flow has shifted by about 30 days, and Monirul Qader Mirza (2003) has identified the significant consequences of peak synchronization on floods in Bangladesh.
- **How will flood timing and mangitude affect crops?** The ultimate effects of floods depend largely on their timing in the crop cycle, and agriculture in general will mediate many of the effects of floods (Mirza et al., 2002). Can this be reframed as a story about the human consequences of flooding, rather than the natural phenomenon?
- **Can the glaciation area affect be incorporated in the model?** Kaser et al. (2003) shows that glaciation can smooth precipitation peaks on a yearly level. If the same is true of large storms, then glaciation might currently be mitigating flood risk, and that effect will decrease as glaciers retreat.

6.2. Unanswered Questions.

- Is there a qualitative difference between large streamflows and catastrophic floods?
- Do I need detailed information about monsoons and the structure of hydrological basins into a model of flood probability?
- How many people are "affected" by seasonal flooding?

6.3. Avenues for Improvements.

- Use a civil hydrological model of the Pakistan basin.
- Build in elements of the diagrams in figure 19 and figure 20.

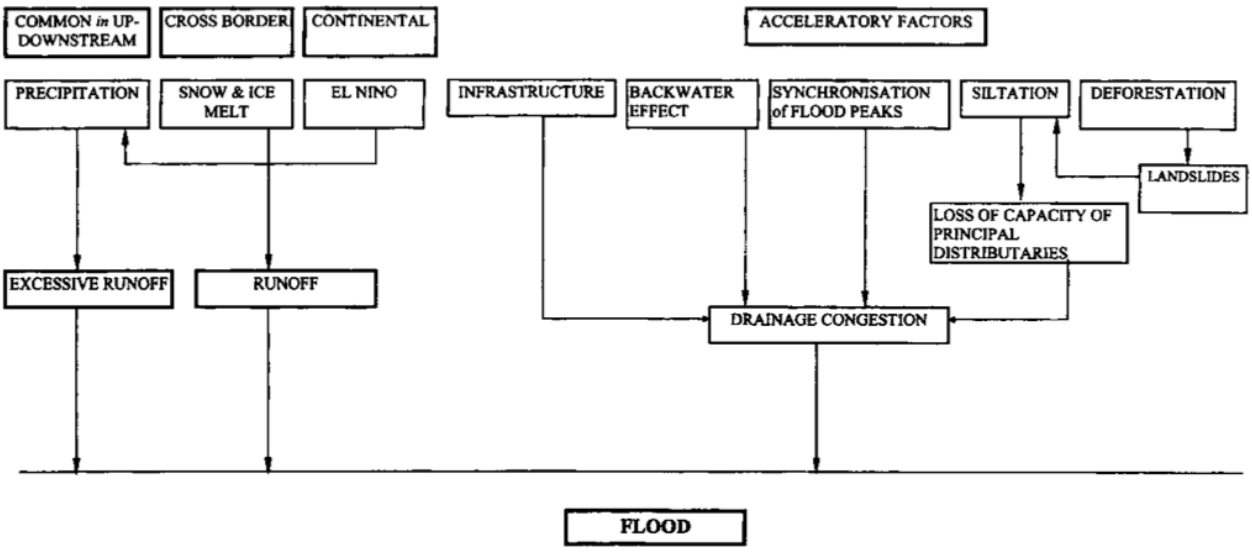

Figure 19: *Causes of Floods:* From Monirul Qader Mirza (2003).

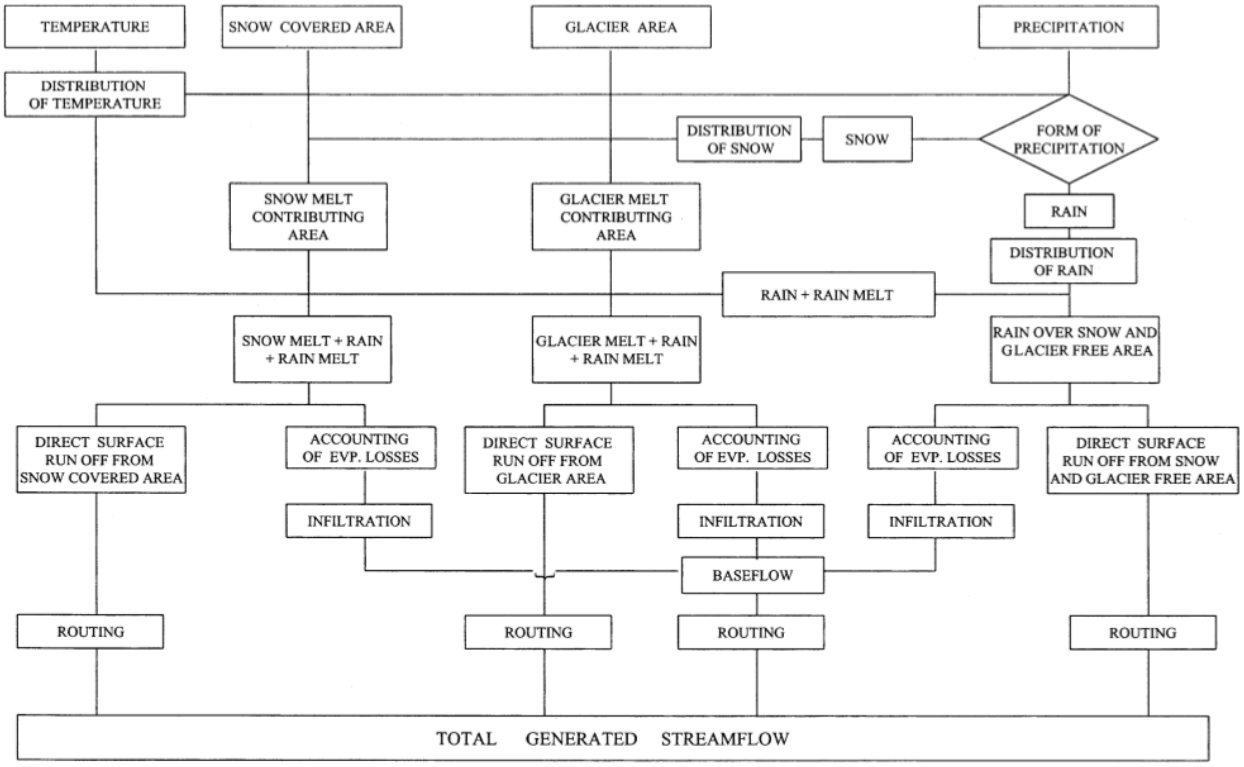

Figure 20: *Causes of Streamflow:* From Singh and Bengtsson (2005).

References

Ageta, Y. (1983). Characteristics of mass balance of the summer-accumulation type glacier in the Nepal Himalaya-I. *Seppyo*, 45(2):81–105.

Ahern, M., Kovats, R., Wilkinson, P., Few, R., and Matthies, F. (2005). Global health impacts of floods: epidemiologic evidence. *Epidemiologic Reviews*, 27(1):36.

Barnett, T., Adam, J., and Lettenmaier, D. (2005). Potential impacts of a warming climate on water availability in snow-dominated regions. *Nature*, 438(7066):303–309.

Cenderelli, D. and Wohl, E. (2001). Peak discharge estimates of glacial-lake outburst floods and "normal" climatic floods in the Mount Everest region, Nepal. *Geomorphology*, 40(1-2):57–90.

Cross, S. R. (2010). Pakistan Floods: The Deluge of Disaster - Facts & Figures as of 15 September 2010. `http://www.reliefweb.int/rw/rwb.nsf/db900SID/LSGZ-89GD7W?OpenDocument`, retrieved December 4, 2010.

Cruz, R., Harasawa, H., Lal, M., Wu, S., Anokhin, Y., Punsalmaa, B., Honda, Y., Jafari, M., Li, C., and Ninh, N. H. (2007). Asia.

Dairaku, K., Emori, S., and Nozawa, T. (2008). Impacts of global warming on hydrological cycles in the Asian monsoon region. *Advances in Atmospheric Sciences*, 25(6):960–973.

Desloges, J. and Church, M. (1992). Geomorphic implications of glacier outburst flooding: Noeick River valley, British Columbia. *Canadian Journal of Earth Sciences*, 29(3):551–564.

Dyurgerov, M., Meier, M., University of Colorado, B. I. o. A., and Research, A. (2005). *Glaciers and the changing Earth system: a 2004 snapshot*. Institute of Arctic and Alpine Research, University of Colorado Boulder.

Farooqi, A., Khan, A., and Mir, H. (2005). Climate change perspective in Pakistan. *Pakistan Journal of Meteorology Vol*, 2(3).

Fujita, K. and Ageta, Y. (2000). Effect of summer accumulation on glacier mass balance on the Tibetan Plateau revealed by mass-balance model. *Journal of Glaciology*, 46(153):244–252.

Fujita, K., Nakawo, M., Fujii, Y., and Paudyal, P. (1997). Changes in glaciers in hidden valley, Mukut Himal, Nepal Himalayas, from 1974 to 1994. *Journal of Glaciology*, 43(145):583–588.

Fujita, K., Ohta, T., and Ageta, Y. (2007). Characteristics and climatic sensitivities of runoff from a cold-type glacier on the Tibetan Plateau. *Hydrological Processes*, 21(21):2882–2891.

Gumbel, E. (1941). The return period of flood flows. *The Annals of Mathematical Statistics*, 12(2):163–190.

Higashi, H., K. D. and Matuura, T. (2006). Impacts of global warming on heavy precipitation frequency and flood risk. *Journal of Hydroscience and Hydraulic Engineering*, 50:205–210.

Hock, R. (2003). Temperature index melt modelling in mountain areas. *Journal of Hydrology*, 282(1-4):104–115.

Huang, M. (1990). On the temperature distribution of glaciers in China. *Journal of Glaciology*, 36(123):210–215.

Kaser, G., Juen, I., Georges, C., Gómez, J., and Tamayo, W. (2003). The impact of glaciers on the runoff and the reconstruction of mass balance history from hydrological data in the tropical Cordillera Blanca, Peru. *Journal of Hydrology*, 282(1-4):130–144.

Kattelmann, R. (2003). Glacial Lake Outburst Floods in the Nepal Himalaya: A Manageable Hazard? *Natural Hazards*, 28(1):145–154.

Kayastha, R., Ageta, Y., Nakawo, M., Fujita, K., Sakai, A., and Matsuda, Y. (2003). Positive degree-day factors for ice ablation on four glaciers in the Nepalese Himalayas and Qinghai-Tibetan Plateau. *Bulletin of glaciological research*, 20:7–14.

Kidson, R. and Richards, K. (2005). Flood frequency analysis: assumptions and alternatives. *Progress in Physical Geography*, 29(3):392.

Kundzewicz, Z. and Takeuchi, K. (1999). Flood protection and management: quo vadimus?/Protection et aménagement contre les inondations: quo vadimus? *Hydrological Sciences Journal*, 44(3):417–432.

Maidment, D. and Koch, M. (1993). *Handbook of hydrology*. McGraw-Hill New York.

Mirza, M. et al. (2002). Global warming and changes in the probability of occurrence of floods in Bangladesh and implications. *Global Environmental Change*, 12(2):127–138.

Mirza, M., Warrick, R., and Ericksen, N. (2003). The implications of climate change on floods of the Ganges, Brahmaputra and Meghna rivers in Bangladesh. *Climatic Change*, 57(3):287–318.

Monirul Qader Mirza, M. (2003). Three recent extreme floods in Bangladesh: a hydro-meteorological analysis. *Natural Hazards*, 28(1):35–64.

Ohmura, A. (2001). Physical basis for the temperature-based melt-index method. *Journal of Applied Meteorology*, 40(4):753–761.

Parry, M. (2007). *Climate Change 2007: impacts, adaptation and vulnerability: contribution of Working Group II to the fourth assessment report of the Intergovernmental Panel on Climate Change*. Cambridge Univ Pr.

Richardson, S. and Reynolds, J. (2000). An overview of glacial hazards in the Himalayas. *Quaternary International*, 65:31–47.

Singh, P. and Bengtsson, L. (2005). Impact of warmer climate on melt and evaporation for the rainfed, snowfed and glacierfed basins in the Himalayan region. *Journal of Hydrology*, 300(1-4):140–154.

Singh, P. and Kumar, N. (1997). Impact assessment of climate change on the hydrological response of a snow and glacier melt runoff dominated Himalayan river. *Journal of Hydrology*, 193(1-4):316–350.

Solomon, S. et al. (2007). *Climate change 2007: the physical science basis*. Cambridge University Press Cambridge.

Todorovic, P. and Zelenhasic, E. (1970). A stochastic model for flood analysis. *Water Resources Research*, 6(6):1641–1648.

Wescoat Jr, J. (1991). Managing the Indus River basin in light of climate change:: Four conceptual approaches. *Global Environmental Change*, 1(5):381–395.

Zimmermann, M., Bichsel, M., and Kienholz, H. (1986). Mountain hazards mapping in the Khumbu Himal, Nepal, with prototype map, scale 1: 50,000. *Mountain Research and Development*, 6(1):29–40.